

Effect of summertime wind conditions on lateral and bottom melting in the central Arctic

Jun INOUE, Takashi KIKUCHI

*Institute of Observational Research for Global Change, Japan Agency for Marine–Earth Science and Technology,
2-15 Natsushima-cho, Yokosuka 237-0061, Japan
E-mail: jun.inoue@jamstec.go.jp*

ABSTRACT. To understand the role of wind conditions on the summertime surface ocean system, the ocean, ice and atmosphere in the central Arctic Ocean were observed using two drifting buoys, one in 2002 under stormy conditions, one in 2003 under calm conditions. Although the ice concentration near the North Pole was the same in 2002 and 2003 during early summer, the heat used in bottom melting in 2003 was only about half of that in 2002. To obtain the total heat input into the upper ocean, heat used in lateral melting was additionally derived from a time series of ice concentration in 2002. Assuming the same heat input into the upper ocean, the heat used in lateral and bottom melting was estimated and compared between the years. It is thought that the warm fresh water embedded within the ice cover was mixed downward during the frequently stormy mid-summer of 2002, enhancing bottom melting. By contrast, the warm water in 2003 tended to be used for lateral melting due to the relatively calm conditions, suggesting that a continuously weak wind favours ice-cover decrease during summer. A simple calculation of the ice-cover evolution reveals that the difference in ice concentration during August between 2002 and 2003 reached 10%, which is consistent with the satellite-derived ice concentration.

INTRODUCTION

The Arctic summer is characterized by the presence of shortwave radiation. The interaction between sea ice and heat input into the upper ocean through the ice–albedo feedback mechanism is one of the most important processes for understanding the Arctic climate. Shortwave radiation penetrating into open water can become a dominant heat source to warm surface ocean waters and subsequently melt the lateral and bottom adjacent sea ice (Maykut and Perovich, 1987; Maykut and McPhee, 1995). Data from a drifting buoy (McPhee and others, 2003) showed that the storage and release of heat obtained from incoming shortwave radiation in the ocean boundary layer during summer dominated the heat flux below the Arctic sea ice. A rapid increase in melt rate in late summer is linked to a build-up of heat in the water, in addition to a sharp increase in floe speed (Perovich and others, 2003).

The deepening of an ocean mixed layer is partly induced by an intense flux of kinetic energy, caused by enhanced air–sea or ice–water stress. This type of mixing is more effective than convective mixing in areas where the stratification near the surface is very stable, such as the Arctic Ocean. A key parameter for this is wind speed. Using Arctic drifting buoys, Yang and others (2004) showed that all mixing events reaching the depth of the halocline were forced by intense storms. Studying the climatology and interannual variability of Arctic cyclone activity, Zhang and others (2004) found that cyclones in the Arctic region tended to be more intense, shorter-lived and fewer in number during winter, while they were less intense, longer-lived and more numerous in summer.

With calm winds, a warm freshwater layer develops at the surface of leads (Richter-Menge and others, 2001), which influences the lateral-melt rate and open-water formation when a local heat balance is maintained (Perovich and others, 2003). During storm-driven strong winds, the heat

stored in the surface layer is transported downward more effectively and forms a well-mixed layer, enhancing bottom melting. Using an ice–ocean coupled single column model, Holland (2003) also verified the importance of heat embedded within summertime leads. However, these studies focused on a very short period (e.g. a few days). Therefore, the relationship between the wind field and the upper ocean system during the Arctic summer as a whole is still poorly understood.

This study examines how the wind speeds affect the heat distribution between the near-surface and mixed layers using observed winds, ice drift, water temperature and ice concentration along the buoy tracks. The data we discuss were obtained primarily by the JAMSTEC (Japan Agency for Marine–Earth Science and Technology) Compact Arctic Drifter (hereafter J-CAD) ice-drifting buoys.

OBSERVATIONS

JAMSTEC has deployed J-CAD buoys near the North Pole as part of the North Pole Environmental Observatory (NPEO) project every year since 2000 (Morison and others, 2002). Recent oceanographic results have highlighted the heat flux under the Arctic sea ice (McPhee and others, 2003), the evolution of the cold halocline layer (Kikuchi and others, 2004b) and the Atlantic Water circulation (Kikuchi and others, 2005), while meteorological results have concentrated on the shortwave radiation and ice–albedo feedback (Inoue and others, 2005). The details of J-CAD buoy technology, data sampling in the Arctic Ocean and data processing are described in Hatakeyama and Monk (2001), Kikuchi and Hosono (2004) and Kikuchi and others (2004a). The J-CAD buoys sample a broad suite of oceanographic (temperature, salinity and currents) and atmospheric (air temperature, wind speed and direction, and air pressure) parameters once per hour. Buoy position is determined by

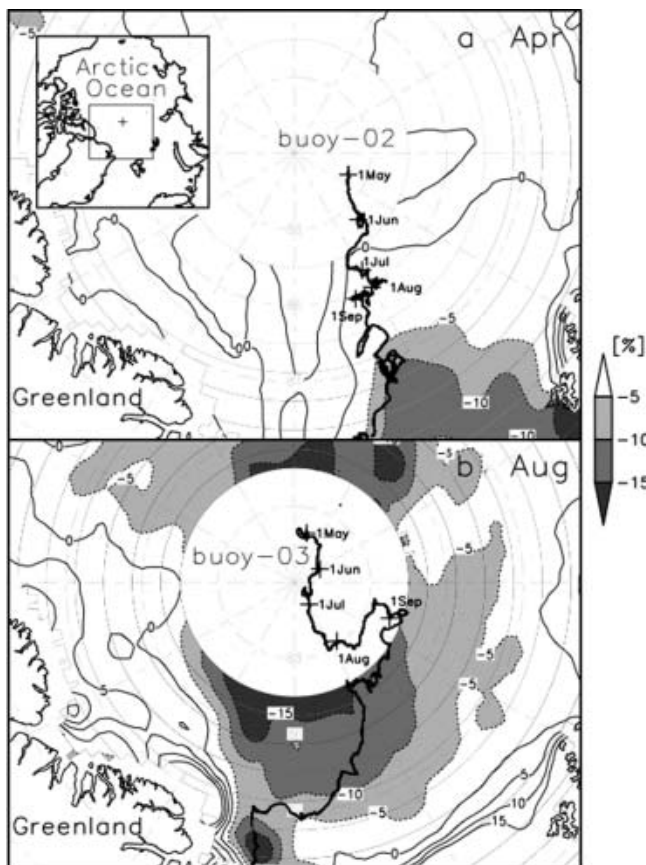


Fig. 1. Drifting trajectory for (a) buoy-02 and (b) buoy-03. The contours and shaded area denote the anomaly (2003 relative to 2002) of the ice concentration derived from SSM/I for (a) April and (b) August. A negative value means that the ice concentration in 2003 is lower than that in 2002.

the global positioning system (GPS), and data are telemetered using the Argos and ORBCOMM systems (Hatakeyama and Monk, 2001).

This work uses data from two J-CADs, deployed in 2002 (hereafter buoy-02) and in 2003 (hereafter buoy-03), to examine the conditions of the upper ocean and the meteorological conditions in the central Arctic. Buoy-02 was installed near the North Pole on 26 April 2002 (88.51° N, 76.93° E; Fig. 1a), and buoy-03 was deployed on 28 April 2003 (88.59° N, 167.38° E; Fig. 1b). The buoys drifted slowly southward from their deployment. By the end of March for each year, they exited the Arctic through the Fram Strait.

Table 1. Wind and the wind factor during mid- (June and July) and late (August and September) summer in 2002 (buoy-02) and 2003 (buoy-03)

Year	Wind		Wind factor	
	Mid-summer m s ⁻¹	Late summer m s ⁻¹	Mid-summer %	Late summer %
2002	4.9	4.0	2.1	2.7
2003	3.9	4.9	2.0	2.6

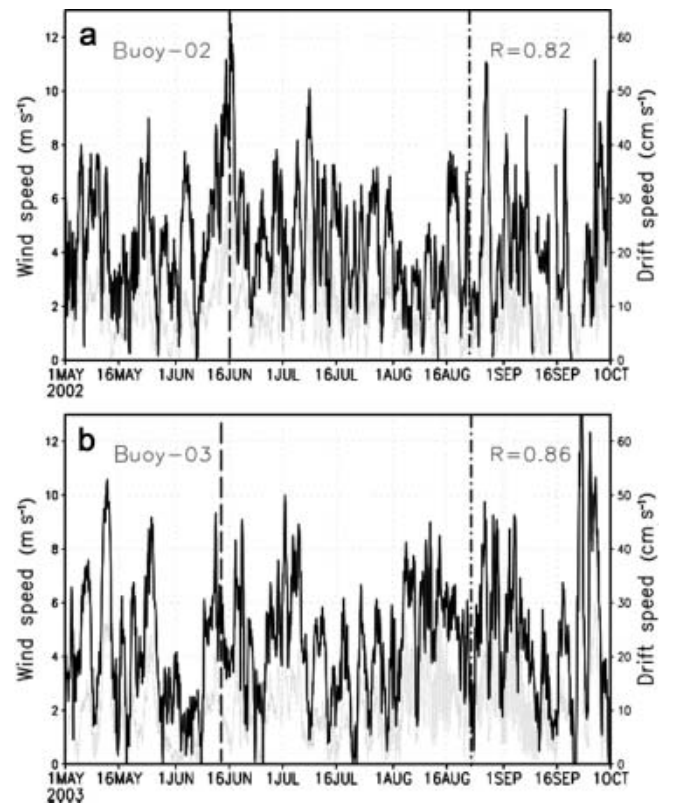


Fig. 2. Time series of wind (black curve) and ice-drift speed (gray curve) for (a) buoy-02 and (b) buoy-03. R is the correlation coefficient between the wind and drift speeds during mid-summer. Dashed and dot-dashed lines denote the melt and freeze onsets, respectively.

In addition to buoy data, ice concentration data derived from the US Defense Meteorological Satellite Program DMSP-F13 Special Sensor Microwave Imager (SSM/I) (D.J. Cavalieri and others, <http://nsidc.org/data/nsidc-0002.html>) were obtained from the US National Snow and Ice Data Center (NSIDC). Figure 1a shows the anomaly of ice concentration in April between 2002 and 2003 (2003 relative to 2002; a negative anomaly means a smaller ice concentration in 2003). The anomaly between the two years is slight in the central Arctic, suggesting that the ice concentration was very similar in both years. By contrast, the difference in August (Fig. 1b) exceeded 10%, suggesting that the area of ice melt in 2003 was larger than in 2002.

RESULTS

Time series of wind and ice-drift speeds for both years are shown in Figure 2. The observation periods are divided into mid- (June and July) and late summer (August and September) for convenience. The wind and drift speeds were well correlated. The wind speed in mid-summer at buoy-02 was stronger than that at buoy-03, and the opposite in late summer (Table 1). The ratio of drift speed to wind speed (the wind factor) increased after August in both years (Table 1). A small wind factor in mid-summer suggests that the ice concentration near the North Pole was high in both years, while a larger wind factor in late summer means that the ice floe had reached a state of free drift, i.e. relatively low ice concentration (Leppäranta, 2005). The dates of melt and freeze onsets defined by Rigor and others (2000), i.e. a

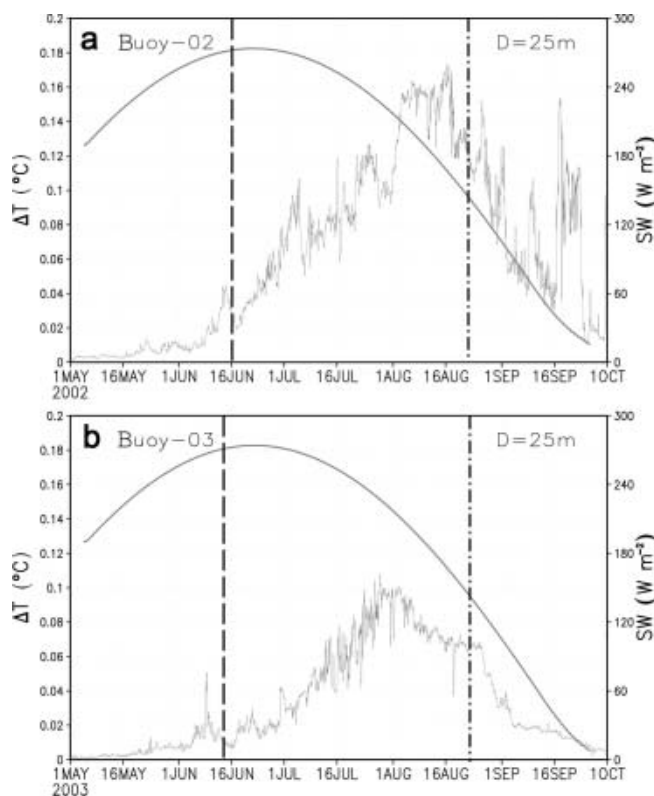


Fig. 3. Time series of temperature above the freezing point at 25 m depth (black curve) and half-value of shortwave radiation at the top of the atmosphere (gray curve) for (a) buoy-02 and (b) buoy-03. Dashed and dot-dashed lines denote the melt and freeze onsets, respectively.

14 day running mean of the 2 m air temperature and a -1°C threshold for the melt season, were also approximately the same in both years (dashed and dot-dashed lines in Fig. 2): 16 June 2002 and 14 June 2003 for melt onset, and 21 August 2002 and 22 August 2003 for freeze onset. These results indicate that the ice and atmospheric conditions around the buoy locations were similar in the two years, except for the wind fields.

Figure 3 shows the evolution of water temperature above the freezing point (ΔT) at 25 m depth along the buoy tracks. Generally, the temperatures began to increase after melt onset, and to decrease after freeze onset. The maximum ΔT was 0.16°C and 0.10°C for 2002 and 2003, respectively, and lagged behind the solar zenith by about 2 months (gray line in Fig. 3). Using a sensible-heat-flux (F_{SH}) parameterization at an ice–water interface (McPhee and others, 2003), heat utilized for bottom melting can be estimated as $F_{\text{SH}} = c_p \rho_w c_h u_{*0} \Delta T$, where c_p is the specific heat of sea water ($4185 \text{ J kg}^{-1} \text{ K}^{-1}$), ρ_w is the density of water (1027 kg m^{-3}), c_h is a bulk heat-transfer coefficient (0.0057) and u_{*0} is the interface friction velocity (0.0056 m s^{-1}). Figure 4 plots the heat used in bottom melting (Q_{bot} in MJ m^{-2}) by accumulating F_{SH} . The heat loss by the bottom melting was 116 and 60 MJ m^{-2} for 2002 and 2003 at the end of September, respectively. This large difference directly corresponds to the difference in a decrease of ice thickness, i.e. 0.36 and 0.19 m for 2002 and 2003, respectively (see right axis in Fig. 4). This decrease of ice thickness in 2002 was consistent with that observed (Inoue and others, 2005) (data for 2003 not available).

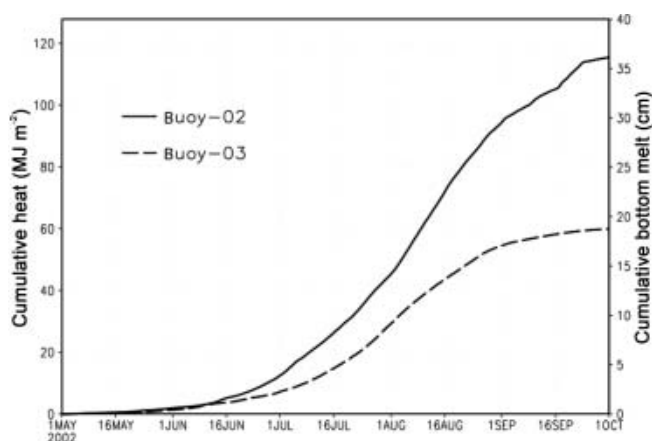


Fig. 4. Time series of cumulative heat used in bottom melting for buoy-02 (solid curve) and buoy-03 (dashed curve). The ordinate on the righthand side represents the corresponding cumulative bottom melt.

Due to the polar gap, satellite-derived ice concentrations at the buoy position are available only for 2002. The temporal evolution of ice concentration averaged in an area of $75 \times 75 \text{ km}^2$ is shown in Figure 5 (gray line). Although the amount of ice cover fluctuated, the value generally decreased from near 100% to 90%, suggesting that lateral melting occurs even in areas that are primarily ice-covered. The heat loss from lateral melting (Q_{lat} in MJ m^{-2}) can be estimated as $Q_{\text{lat}} = \rho_i L_f H \Delta A_i$, where ρ_i is the density of ice (900 kg m^{-3}), L_f is the latent heat of fusion for sea ice (0.355 MJ kg^{-1}), H is the ice thickness (2.5 m), and ΔA_i is the decrease in ice cover during the summer (8%). The estimated heat loss is 64 MJ m^{-2} , which is about half of Q_{bot} in 2002.

Under the same conditions of ice concentration (Fig. 1a) and shortwave radiation, the heat loss by lateral melting in 2003 was also estimated as the residual term. Table 2 summarizes the heat used for lateral melting (Q_{lat}) and bottom melting (Q_{bot}) for each buoy. In 2003, Q_{lat} amounts to about 67% of the heat input, which presumably enhances the decrease in ice cover, while in 2002, Q_{lat} (36%) is

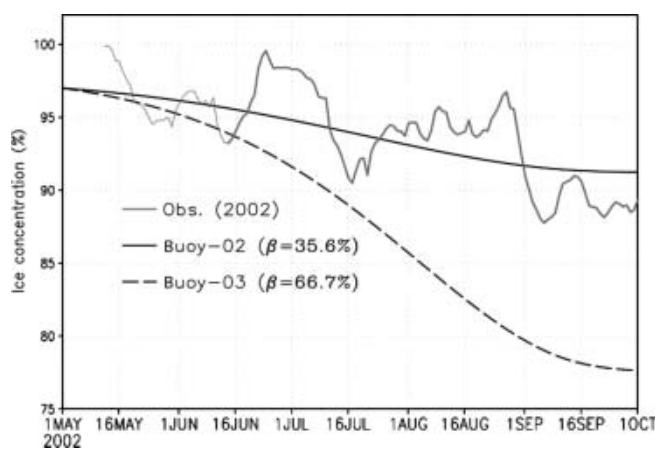


Fig. 5. Evolution of ice concentration calculated from different lateral melting rates for buoy-02 (solid black curve) and buoy-03 (dashed curve), and observed by SSM/I at the nearest buoy position (solid gray curve). Data affected by the polar gap are denoted by a thin gray curve.

Table 2. Heat utilized for lateral and bottom melting (MJ m^{-2})

Year	Q_{lat}	Q_{bot}
2002	64 (35.6%)	116 (64.4%)
2003	120 (66.7%)*	60 (33.3%)

*Indirect estimate.

smaller due to the relatively large contribution of Q_{bot} (64%). The difference in the heat distribution into the upper ocean likely caused the significant anomaly of the ice concentration in August, as shown in Figure 1b.

To understand the effect of the heat stored in the surface layer on the lateral melting, the evolution of the ice concentration from May to October was calculated. The simplest case was assumed: all solar energy absorbed is immediately used for lateral melting, and any change in ice thickness is negligible. For such a case, the following simple relationship is satisfied: $F_0 = \beta A_w (1 - \alpha) F_{\text{SW}} = \rho_i L_f H (dA_w/dt)$, where F_0 is the amount of heat stored in a unit area of the surface ocean system, β is the proportion of heat absorbed in the surface layer (Table 2), and α is the albedo of water (0.1). The area of open water, A_w , at the initial time ($t = 0$) was adjusted to 3%, corresponding to ice concentrations of $A_i = 97\%$, to reproduce the evolution of the observed ice concentration. The daily mean shortwave radiation (F_{SW}) at the surface at the buoy position for 2002 was given as the half-value of the daily mean shortwave radiation at the top of the atmosphere (Fig. 3a). Inoue and others (2005) verified this assumption. The sensitivity of β was determined for the 2002 ($\beta = 35.6\%$) and 2003 ($\beta = 66.7\%$) cases. The temporal evolution of the modelled ice concentration is shown in Figure 5 for both cases. It is clear that the difference in the ice cover increases in late summer. The anomaly between the two cases reached about 10% in August.

DISCUSSION

To investigate ice–ocean heat exchange in polar leads, Skillingstad and others (2005) conducted a large-eddy simulation coupled to a slab ice model, and demonstrated that lateral melting rates decreased under stronger-wind conditions due to greater turbulent mixing of cold water from beneath the fresh layer embedded with sea ice. They also mentioned that a number of sea-surface wind events of $6\text{--}7 \text{ m s}^{-1}$ evidently caused the newly formed fresh layer to weaken or entirely mix out, while heat loss through entrainment into the mixed layer was not greatly increased up to 5 m s^{-1} . Because our wind speed was observed on the ice with relatively large friction, the apparent threshold wind speed to initiate the turbulent mixing would be smaller than 5 m s^{-1} . Therefore, the difference in the wind speeds between 2002 (4.9 m s^{-1}) and 2003 (3.9 m s^{-1}) during mid-summer might be significant for the turbulent heat-exchange processes.

This idea can also be applied to explain a difference in the decrease in water temperature around the freeze onset. At buoy-02, the temperature after the freeze onset decreased in steps, in association with relatively short, strong-wind events as on 29 August and 2–5 September (Figs 2a and 3a). These events affected vertical mixing with the downward transport of melted cold fresh water below the ice. In contrast, at

buoy-03, there is presumably less meltwater under the sea ice because lateral melting was predominant in mid-summer. Therefore, even if strong-wind events occur in late summer, as in mid-August 2003, the decrease in temperature is small (Figs 2b and 3b). However, once the warm water embedded within leads spreads out below the ice, which promotes bottom melting (Fig. 4), the same cooling and freshening events occur within the mixed layer during strong-wind conditions, as at the end of August 2003 (Fig. 3b).

CONCLUSION

Data from buoys deployed near the North Pole as part of the NPEO project were analyzed for a relatively windy summer in 2002 (buoy-02) and a calm summer in 2003 (buoy-03). For better understanding the role of wind speed on the summertime upper ocean system, the heat used in bottom melting was calculated from the water temperature observed by each buoy: the heat at buoy-03 (60 MJ m^{-2}) was about half of that at buoy-02 (116 MJ m^{-2}). To obtain the total heat input into the upper ocean, the heat used in lateral melting was also estimated using a time series of ice concentration for buoy-02 (64 MJ m^{-2}). Since the meteorological situation and ice concentration between the years were similar, except for wind speeds, the heat used in lateral melting at buoy-03 was calculated (120 MJ m^{-2}) as the residual term from the total heat input for buoy-02 and the heat used in bottom melting at buoy-03. The heat distribution at buoy-03 was characterized by the heat used in lateral melting at the near surface within the leads (about 65% of the total heat input) due to relatively calm wind conditions, whereas at buoy-02 it was characterized by the large heat input below the ice (about 65%) due to relatively windy conditions. The effect of this difference on the ice extent in late summer was demonstrated using a simple model of the evolution of sea ice. The result was consistent with the anomaly (10%) of the satellite-derived ice concentration in late summer, which emphasizes the importance of heat in leads to the sea-ice melting. To adequately model the ocean–ice–atmosphere coupling system, the treatment of wind fields near the surface, as well as the sub-gridscale parameterization of warm water embedded within ice cover, will be necessary.

ACKNOWLEDGEMENTS

We sincerely thank all participants in the NPEO buoy deployments. We are deeply indebted to M. Hosono of JAMSTEC and K. Kato of International Meteorological and Oceanographic Consultants Co., Ltd for help with the J-CAD data processing. We were helped by discussions with J.H. Morison, and the suggestions and comments of the scientific editor, P. Heil, and reviewers. The SSM/I data were provided by the NSIDC, University of Colorado. Project support was provided by JAMSTEC and US National Science Foundation grants OPP-9910305 and OPP-0352754.

REFERENCES

- Hatakeyama, K. and T. Monk. 2001. Development and deployment of a compact Arctic drifting platform. *Sea Technol.*, **42**(7), 37–47.
- Holland, M.M. 2003. An improved single-column model representation of ocean mixing associated with summertime leads: results from a SHEBA case study. *J. Geophys. Res.*, **108**(C4), 3107. (10.1029/2002JC001557.)

- Inoue, J., T. Kikuchi, D.K. Perovich and J.H. Morison. 2005. A drop in mid-summer shortwave radiation induced by changes in the ice-surface condition in the central Arctic. *Geophys. Res. Lett.*, **32**(13), L13603. (10.1029/2005GL023170.)
- Kikuchi, T. and M. Hosono. 2004. JAMSTEC Compact Arctic Drifter Buoy Data. *CliC Ice Climate News*, **5**, 14–15.
- Kikuchi, T., M. Uno, M. Hosono and K. Hatakeyama. 2004a. Accurate ocean current observation near the magnetic dip pole: compass error estimation. *J. Jpn Soc. Mar. Surv. Technol.*, **16**(1), 19–27. [In Japanese.]
- Kikuchi, T., K. Hatakeyama and J.H. Morison. 2004b. Distribution of convective Lower Halocline Water in the eastern Arctic Ocean. *J. Geophys. Res.*, **109**(C12), C12030. (10.1029/2003JC002223.)
- Kikuchi, T., J. Inoue and J.H. Morison. 2005. Temperature difference across the Lomonosov Ridge: implications for the Atlantic Water circulation in the Arctic Ocean. *Geophys. Res. Lett.*, **32**(20), L20604. (10.1029/2005GL023982.)
- Leppäranta, M. 2005. *The drift of sea ice*. Berlin, etc., Springer-Verlag.
- Maykut, G.A. and M.G. McPhee. 1995. Solar heating of the Arctic mixed layer. *J. Geophys. Res.*, **100**(C12), 24,691–24,703.
- Maykut, G.A. and D.K. Perovich. 1987. The role of shortwave radiation in the summer decay of a sea ice cover. *J. Geophys. Res.*, **92**(C7), 7032–7044.
- McPhee, M.G., T. Kikuchi, J.H. Morison and T.P. Stanton. 2003. Ocean-to-ice heat flux at the North Pole environmental observatory. *Geophys. Res. Lett.*, **30**(24), 2274. (10.1029/2003GL018580.)
- Morison, J.H. and 10 others. 2002. North Pole environmental observatory delivers early results. *EOS Trans. AGU*, **83**(33), 357, 360–361.
- Perovich, D.K., T.C. Grenfell, J.A. Richter-Menge, B. Light, W.B. Tucker, III and H. Eicken. 2003. Thin and thinner: ice mass balance measurements during SHEBA. *J. Geophys. Res.*, **108**(C3), 8050. (10.1029/2001JC001079.)
- Richter-Menge, J.A., D.K. Perovich and S. Pegau. 2001. Summer ice dynamics during SHEBA and its effect on the ocean heat content. *Ann. Glaciol.*, **33**, 201–206.
- Rigor, I.G., R.L. Colony and S. Martin. 2000. Variations in surface air temperature observations in the Arctic, 1979–97. *J. Climate*, **13**(5), 896–914.
- Skyllingstad, E.D., C.A. Paulson and W.S. Pegau. 2005. Simulation of turbulent exchange processes in summertime leads. *J. Geophys. Res.*, **110**(C5), C05021. (10.1029/2004JC002502.)
- Yang, J., J. Comiso, D. Walsh, R. Krishfield and S. Honjo. 2004. Storm-driven mixing and potential impact on the Arctic Ocean. *J. Geophys. Res.*, **109**(C4), C04008. (10.1029/2001JC001248.)
- Zhang, X., J.E. Walsh, J. Zhang, U.S. Bhatt and M. Ikeda. 2004. Climatology and interannual variability of Arctic cyclone activity: 1948–2002. *J. Climate*, **17**(12), 2300–2317.